



Filled skutterudite superconductor $\text{CaOs}_4\text{P}_{12}$ prepared by high-pressure synthesis

メタデータ	言語: English 出版者: American Physical Society 公開日: 2018-08-17 キーワード (Ja): キーワード (En): 作成者: 川村, 幸裕, 出南, 真吾, SALAMAKHA, Leonid, SIDORENKO, Andrey, HEINRICH, Patrick, MICHOR, Herwig, BAUER, Ernst, 関根, ちひろ メールアドレス: 所属:
URL	http://hdl.handle.net/10258/00009674

Filled skutterudite superconductor $\text{CaOs}_4\text{P}_{12}$ prepared by high-pressure synthesis

Yukihiro Kawamura¹, Shingo Deminami¹, Leonid Salamakha², Andrey

Sidorenko², Patrick Heinrich², Herwig Michor², Ernst Bauer², Chihiro Sekine¹

¹*Muroran Institute of Technology, Mizumoto 27-1, Muroran, Hokkaido 050-8585, Japan*

²*Institute of Solid State Physics, TU Wien, Wiedner Hauptstraße 8-10, A-1040 Vienna, Austria*

(Dated: August 10, 2018)

In this paper, we report the transport, thermodynamic, and superconducting properties of a new filled skutterudite $\text{CaOs}_4\text{P}_{12}$ synthesized under high pressure and high temperature. The electrical resistivity of 3.4–4.8 m Ωcm , carrier concentration of $3.8\text{--}6.1 \times 10^{20}\text{cm}^{-3}$, and positive Hall coefficient suggest that $\text{CaOs}_4\text{P}_{12}$ is a semimetal with hole carriers. An anomaly due to low-energy optical modes corresponding to an Einstein temperature of 150 K was observed in the specific heat. Resistivity, dc magnetic susceptibility, and specific heat measurements indicate bulk superconductivity below 2.5 K. The specific heat anomaly at T_c , $\Delta C/\gamma T_c \approx 1.4$, is in agreement with the Bardeen-Cooper-Schrieffer (BCS) value of 1.43. The electron-phonon coupling constant λ_{ep} is estimated to be 0.47. $\text{CaOs}_4\text{P}_{12}$ is classified as a BCS-type, weakly coupled type-II superconductor with an upper critical field of $H_{c2} \approx 22$ kOe and Ginzburg-Landau coherence length of $\xi \approx 12$ nm.

PACS numbers: 74.70.Dd, 74.25.Bt, 74.25.fc, 74.25.Ha

I. INTRODUCTION

Filled skutterudite compounds crystallize in a cubic crystal structure with the space group $\text{Im}\bar{3}$ (No. 204) [1] and are denoted by the chemical formula AT_4X_{12} (A = alkali metal, alkaline earth metal, rare earth metal, or actinide; T = Fe, Ru, Os, Co, Rh, Ir, Pt; X = P, As, Sb, Ge). They exhibit a wide variety of strongly correlated electron phenomena, such as the metal-insulator transition in $\text{PrRu}_4\text{P}_{12}$ [2], non-Fermi liquid behavior in $\text{CeRu}_4\text{Sb}_{12}$ [3], multipole ordered states in $\text{SmRu}_4\text{P}_{12}$ [4], and heavy fermion and multipolar ordering in $\text{PrFe}_4\text{P}_{12}$ [5, 6].

Although most of these characteristic behaviors are observed in AT_4X_{12} compounds where the element of the A site is in a trivalent state, the A site element can be monovalent, divalent, or tetravalent as well. In fact, superconductivity has been found with divalent or trivalent A states in AT_4X_{12} . There are some unique superconductors corresponding to the trivalent state of the A site in AT_4X_{12} . $\text{PrOs}_4\text{Sb}_{12}$, exhibiting strong-coupling superconductivity below $T_c \approx 1.85$ K, breaks time-reversal symmetry in its superconducting states with several distinct superconducting phases [7]. $\text{LaFe}_4\text{P}_{12}$ with $T_c \approx 4.1$ K and $\text{YFe}_4\text{P}_{12}$ with $T_c \approx 5.6$ K exhibit positive pressure dependencies of T_c [8, 9], contrary to the predictions of the McMillan theory [10, 11]. Although $\text{LaOs}_4\text{P}_{12}$ has been regarded as a simple superconductor, another phase transition around the superconducting transition temperature was observed recently [12]. For a divalent state of the A site in AT_4X_{12} , several alkaline-earth-filled skutterudites, such as $\text{Ba}_{0.85}\text{Ir}_4\text{As}_{12}$, $\text{Ba}_{0.89}\text{Ir}_4\text{P}_{12}$ [13], $\text{SrPt}_4\text{Ge}_{12}$, and $\text{BaPt}_4\text{Ge}_{12}$ [14, 15], have been reported as superconductors.

Some of the filled-skutterudite superconductors, including $\text{Ba}_{0.85}\text{Ir}_4\text{As}_{12}$ and $\text{Ba}_{0.89}\text{Ir}_4\text{P}_{12}$, can only be synthesized at high pressures and high temperatures (HPHTs). The superconductor with the highest criti-

cal temperature among filled skutterudites, $\text{La}_{0.8}\text{Rh}_4\text{P}_{12}$ with $T_c \approx 14.9$ K can also only be synthesized at HPHTs [16]. The HPHT synthesis is an excellent technique to synthesize samples that do not form otherwise at ambient conditions. Recently, we have reported new skutterudite superconductors prepared with this technique, such as $\text{BaOs}_4\text{P}_{12}$ and $\text{SrOs}_4\text{As}_{12}$ [17, 18]. Such alkaline-earth-filled skutterudites are also important for comparison with Eu-filled skutterudites, which are likely to order ferromagnetically. $\text{EuFe}_4\text{As}_{12}$ orders at exceptionally high temperatures, $T_C \approx 152$ K, compared to other isostructural compounds [19], whereas $\text{EuOs}_4\text{P}_{12}$ exhibits a ferromagnetic transition at $T_C \approx 15$ K with an Eu valence of 2+ [20]. To clarify the origin of the exceptionally high T_C of $\text{EuFe}_4\text{As}_{12}$ and the magnetic properties of Eu compounds in general, a comparison with 2+ nonmagnetic A elements is helpful. In addition, superconductivity of $\text{AOs}_4\text{P}_{12}$ (A = alkaline earth metal) might show a unique behavior, as well as that of $\text{LaOs}_4\text{P}_{12}$ because these compounds are expected to be similar. Due to a lower supply of electrons from the A site, the carrier concentration of $\text{AOs}_4\text{P}_{12}$ is expected to be lower than that of $\text{LaOs}_4\text{P}_{12}$.

The following are alkaline-earth-filled skutterudites: AT_4X_{12} (A = Ca, Sr, Ba, T = Fe, Ru, Os, X = P, As, Sb). Sb-based filled skutterudites $AT_4\text{Sb}_{12}$ (A = Ca, Sr, Ba, T = Fe, Ru, Os) except $\text{CaRu}_4\text{Sb}_{12}$, have been reported [21–27]. $\text{AFe}_4\text{Sb}_{12}$ (A =Ca, Sr, Ba) have been reported as nearly ferromagnetic materials with spin fluctuation of Fe 3d electrons [25], while $\text{AOs}_4\text{Sb}_{12}$ (A =Sr, Ba) have a large density of states derived from Os 5d states near the Fermi level with a hint of strong electron-phonon interaction [26]. So far reported $AT_4\text{Sb}_{12}$ compounds show metallic resistivity behavior with a room temperature resistivity $\rho_{300\text{K}} \approx 0.3\text{--}0.6$ m Ωcm , while the Sommerfeld coefficient γ depends on the T site, i.e., $\gamma \approx 90\text{--}120$ mJ/molK² for T = Fe, $\gamma \approx 10$ mJ/molK² for T = Ru, $\gamma \approx 40\text{--}50$ mJ/molK² for T = Os [27]. Among

As-based filled skutterudites, $\text{SrT}_4\text{As}_{12}$ ($T = \text{Fe, Ru, Os}$), and $\text{BaT}_4\text{As}_{12}$ ($T = \text{Fe, Ru}$) have been reported [18, 28–30]. $\text{SrFe}_4\text{As}_{12}$ and $\text{BaFe}_4\text{As}_{12}$ have been reported as nearly ferromagnetic materials and $\text{SrOs}_4\text{As}_{12}$ has been reported as a superconductor below 4.8 K [18, 29]. Their resistivities show metallic temperature dependence with a high value of $\rho_{300\text{K}} \approx 1\text{--}5 \text{ m}\Omega\text{cm}$. As for P-based filled skutterudites, only $\text{BaOs}_4\text{P}_{12}$ has been reported as a superconductor below 1.8 K [17].

In this article, we present the physical properties of a new filled skutterudite $\text{CaOs}_4\text{P}_{12}$ synthesized at HPHT. $\text{CaOs}_4\text{P}_{12}$ is found to be a weakly coupled bulk superconductor and the first superconductor among Ca-filled skutterudites.

II. EXPERIMENTS

$\text{CaOs}_4\text{P}_{12}$ was synthesized at 4 GPa and 1050 °C by the HPHT method using a Kawai-type two-stage anvil apparatus. The starting material was a Ca-rich mixture of elements with Ca (95 %, Wako Junyaku), Os (99.99 % NewMet Koch), and P (99.9999 %, Soekawa Chemical) as $\text{Ca}_{1.3}\text{Os}_4\text{P}_{12}$. The procedure was carried out under an argon atmosphere with an oxygen contamination of less than 5 ppm to prevent the oxidation of Ca. The resulting materials were evaluated by Co-K α x-ray diffraction with powdered silicon as an internal standard. The composition of the obtained material was evaluated by scanning electron microscopy with energy dispersive x-ray spectroscopy (SEM-EDX). The heat capacity was measured using a relaxation method with a commercial physical properties measurement system (PPMS, Quantum Design). The electrical resistivity and Hall effect were measured using the standard four-terminal method with dc current. The magnetization was measured using a superconducting quantum interference device magnetometer. The resistivity was studied under pressure and magnetic fields in a ^3He cryostat with a superconducting magnet. Pressure was applied with a piston-cylinder-type pressure cell with two layers consisting of CuBe and WC. Daphne oil 7373 was used as pressure medium. The absolute value of the pressure was evaluated from the Curie temperature of HoCo_2 as an internal standard [31].

III. RESULTS

A. Sample characterization

The x-ray powder diffraction pattern of the sample synthesized at HPHT is shown in Fig. 1. Almost all distinct peaks can be indexed by the filled skutterudite structure. The lattice parameter of $\text{CaOs}_4\text{P}_{12}$ is calculated to be $8.084 \pm 0.004 \text{ \AA}$. OsP_4 and OsP_2 with less than 4 % of the total intensity are observed as secondary phases. The electron backscattering SEM image is shown in the inset of Fig. 1. The image is composed of four

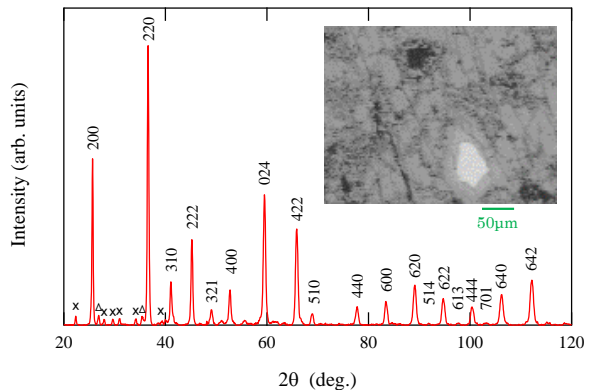


FIG. 1. (Color online) Powder x-ray diffraction results for $\text{CaOs}_4\text{P}_{12}$. All the peaks except the tiny peaks due to impurities can be indexed to the cubic ($\text{Im}\bar{3}$) symmetry. Diffraction indexes have been assigned to each peak, which were used to calculate the lattice parameter. The peaks marked by triangles and crosses are attributed to the secondary phases OsP_2 and OsP_4 , respectively. The inset shows the electron backscattering SEM image.

parts: gray and black areas and a white spot surrounded by a light gray area. According to the point composition analysis (PCA) of each area with EDX, the gray area indicates $\text{CaOs}_4\text{P}_{12}$, while the black area indicates holes, i.e., a void or crack in the sample. The PCA of the gray area also indicates a 5 % variation in Ca and Os in $\text{CaOs}_4\text{P}_{12}$. In addition, the PCA indicates that the white spot and its surrounding light gray area are OsP_2 and OsP_4 , respectively. The presence of these secondary phases is attributable to several factors. One is the HPHT synthetic conditions such as temperature, pressure, and holding time. Although we have optimized the synthetic conditions as 4 GPa, 1050 °C, and 90 min, which are possibly not exactly the optimal parameters. Another is the Ca element impurities. The Ca element impurities, other than Mg (< 0.05 %), indicated by the supplying company, are likely oxygen, nitrogen, and carbon. The formation of OsP_2 or OsP_4 phases, in spite of 30 % Ca surpluses for enhancing the reaction of the Ca element against Os and P elements, might partially be attributed to the presence of such O, N, C impurities. Here, we discuss the effect of these secondary phases on the magnetic and transport properties. From the ratio of areas of the gray, white, and light gray parts of the backscattering SEM image of the whole sample, we can evaluate the approximate phase fractions. The volume fractions of $\text{CaOs}_4\text{P}_{12}$, OsP_2 , and OsP_4 obtained thereby, are 97 %, 1 %, and 2 %, respectively. OsP_2 is reported as a narrow-gap semiconductor with 1.13 eV [32], whereas OsP_4 is reported as a diamagnetic semiconductor [33]. They have barely any effect on the transport properties. This is because these compounds are reported as semiconductors, and are not known as superconductors in the temperature range studied. Moreover, they are aggre-

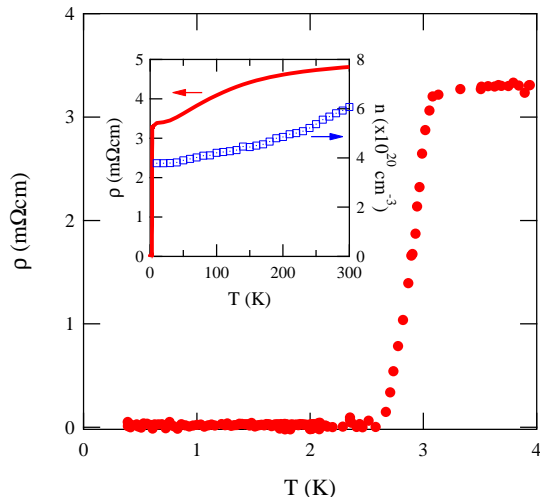


FIG. 2. (Color online) Temperature dependence of the electrical resistivity (ρ) below 4 K. The red line for the left axis of the inset shows $\rho(T)$ up to 300 K. The square symbol for the right axis of the inset shows the carrier concentration n , up to 300 K.

gated into a chunk and not into lines or two-dimensional layers. In addition, OsP₂ and OsP₄ have small effects on the magnetic properties because the volume fractions of these compounds are approximately 3 % in total compared to CaOs₄P₁₂, and both OsP₄ and OsP₂ are diamagnetic.

B. Transport and thermodynamic properties

Figure 2 (inset) illustrates the temperature-dependent electrical resistivity (ρ). ρ monotonically decreases with decreasing temperature without any anomalies down to T_c from room temperature. A drop in $\rho(T)$ below 3.1 K and zero resistivity below 2.6 K are observed, indicating superconductivity with a transition width $\Delta T_c = 0.5$ K. A fit to the normal state resistivity via $\rho(T) = \rho_0 + AT^2$ revealed $\rho_0 = 3.4$ mΩcm and $A = 9.5 \times 10^{-5}$ mΩcm/K². The resistivity above T_c is 3.4–4.8 mΩcm, comparable to the value of ρ with 1.8–3.3 mΩcm of isostructural EuOs₄P₁₂ above the Curie temperature [20]. A measurement of the Hall effect indicates a positive Hall coefficient, revealing holes as predominant charge carriers in CaOs₄P₁₂. The carrier concentration $n = 3.8$ – 6.1×10^{20} cm⁻³ is comparable but higher than that of the isostructural semiconductor CeOs₄P₁₂ because of c-f hybridization ($n = 2 \times 10^{18}$ – 7×10^{19} [34]). The values of ρ and n are in between those of metals and semiconductors. The broad hump of $\rho(T)$ from 50 to 250 K and the semiconducting-like decrease of $n(T)$ despite the metallic decrease of ρ with decreasing temperature, as well as the absolute values of ρ and n suggest that CaOs₄P₁₂ is a semimetal. This is consistent with LaOs₄P₁₂ being a metal because divalent Ca supplies less electrons to the

crystal than trivalent La does.

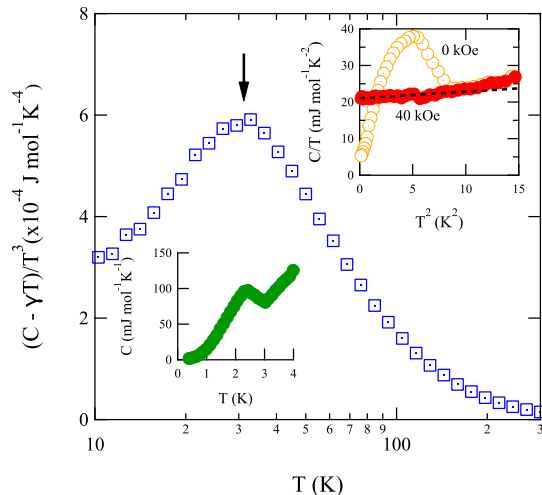


FIG. 3. (Color online) Temperature dependence of the phonon contribution of the specific heat (C) plotted as $(C - \gamma T)/T^3$. The left-bottom inset shows the temperature dependence of C . The top-right inset shows C/T vs. T^2 at zero-field (open circle) and under a field of 40 kOe (filled circle). The dashed line indicates a linear fit.

The left-bottom inset of Fig. 3 illustrates the temperature dependence of the specific heat (C). A distinctive anomaly due to superconductivity is observed below 3 K, which is one piece of evidence of bulk superconductivity of CaOs₄P₁₂. Figure 3 (main panel) shows the temperature dependence of $(C - \gamma T)/T^3$, where γ is the Sommerfeld coefficient. Under a field of 40 kOe, the anomaly due to superconductivity is completely suppressed and the specific heat of CaOs₄P₁₂ obeys $C = \gamma T + \beta T^3$, as shown in the top-right inset of Fig. 3, where βT^3 is the phonon contribution to the specific heat. γ and β of CaOs₄P₁₂ are evaluated by fitting the data of the specific heat between 0.38 and 3 K, and are derived as 21 mJ/molK² and 0.18 mJ/molK⁴, respectively. The Debye temperature Θ_D is derived from $\Theta_D = (12\pi^4/5\beta \cdot nR)^{1/3}$ as 560 K, where $n = 17$ is the number of atoms per formula unit and R is the gas constant. $(C - \gamma T)/T^3$ (T) shows the broad peak at $T_{\max} = 31$ K, a hint of harmonic vibrations (rattling-modes) at the Ca sites of CaOs₄P₁₂ due to low-energy optical modes. The existence of rattling modes, of course, deserves further verification by other signatures like an enhanced displacement parameter observed from crystal structure refinements. This characteristic temperature, described as the Einstein temperature Θ_E , can be estimated by the equation $\Theta_E \approx 4.92 T_{\max}$ [35], as $\Theta_E \approx 150$ K. This value is comparable to the isostructural compounds LaOs₄P₁₂ with $\Theta_E = 131$ K [35]. The guest-free distance, corresponding to the space of the A site, of CaOs₄P₁₂ is comparable to that of LaOs₄P₁₂ because the ionic radius of Ca²⁺ with 1.12 Å is similar to that of La³⁺ with 1.16 Å and the lattice constant of CaOs₄P₁₂ with 8.084 Å is equals to that of LaOs₄P₁₂ with 8.084

Å [1].

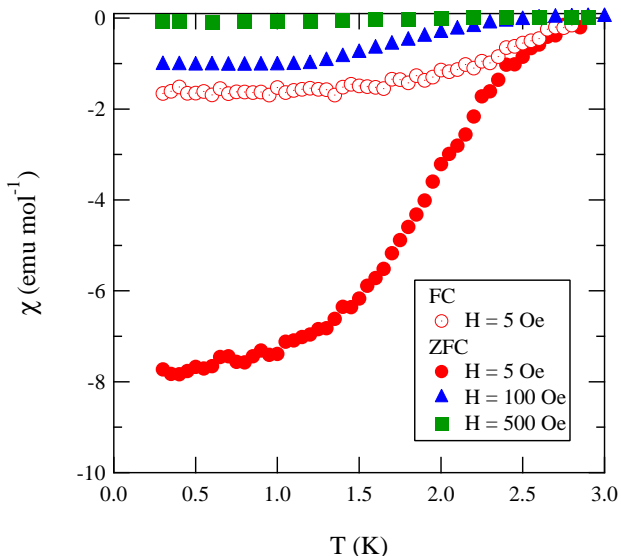


FIG. 4. (Color online) Temperature dependence of the dc magnetic susceptibility of $\text{CaOs}_4\text{P}_{12}$ below 3 K with 5 Oe (filled circle), 100 Oe (filled triangle), and 500 Oe (filled square) after zero field cooling (ZFC) and with 5 Oe after field cooling (FC; open circle).

Figure 4 illustrates the temperature-dependent dc magnetic susceptibility of $\text{CaOs}_4\text{P}_{12}$ below 3 K. The magnetic susceptibility χ , measured at 5 Oe after ZFC, shows the Meissner effect below approximately 3 K, which is the other evidence for $\text{CaOs}_4\text{P}_{12}$ being a bulk superconductor. There is a distinct difference between ZFC and FC, which is characteristic of type-II superconductivity. In a small field of 100 Oe, the diamagnetic susceptibility (χ) is significantly reduced compared to its magnitude measured at the lowest field of 5 Oe, indicating that the lower critical field H_{c1} is relatively small in $\text{CaOs}_4\text{P}_{12}$. The superconducting transition observed in all measurements is not sharp, because of variations in the Ca composition as derived from the SEM-EDX analysis. From the results of $\rho(T)$, $C(T)$, and $\chi(T)$, $\text{CaOs}_4\text{P}_{12}$ exhibits bulk superconductivity below 2.5 K.

C. Superconducting properties

In the following paragraphs, the superconducting properties of $\text{CaOs}_4\text{P}_{12}$ will be discussed in detail. Figure 5 shows the electronic specific heat contribution $C_e(T)$ of $\text{CaOs}_4\text{P}_{12}$. C_e is deduced from $C_e = C - \beta T^3$, where C is the total specific heat. C_e/T shows the residual Sommerfeld coefficient γ_r estimated as 5 mJ/molK² at the lowest temperatures, mostly due to OsP_4 and OsP_2 impurities. The electronic Sommerfeld coefficient of the normal state of the superconductor, γ_s , should be taken into account, i.e., $\gamma_s = \gamma - \gamma_r = 16$ mJ/molK². A clear anomaly related to the superconductivity is observed in

C_e/T . Mühlischlegel presented a generalized data set of specific heat based on the BCS theory [36]. The solid line in Fig. 5 represents the sum of the specific heat of γ_r and that of the data set presented by Mühlischlegel. Considering the entropy balance of the idealized jump at T_c , the thermodynamic superconducting transition temperature can be defined as 2.5 K, as indicated by the arrow in Fig. 5. In the BCS theory, the specific heat ratio at T_c , $\Delta C/\gamma T_c$, takes the value 1.43. With the values used in this study, i.e., $\Delta C = 55$ mJ/molK, $\gamma_s = 16$ mJ/molK², and $T_c = 2.5$ K, the bulk ratio $\Delta C/\gamma_s T_c$ is deduced as 1.4, which is nearly the same value as the prediction for weakly coupling BCS superconductor. When a magnetic field is applied, T_c and the value of $C_e(T)$ at T_c are monotonically suppressed with increasing field.

Here we discuss the Sommerfeld value γ_s that we have deduced. A close correspondence of γ_s of $\text{CaOs}_4\text{P}_{12}$ and $\text{LaOs}_4\text{P}_{12}$ is expected because they share the same P p bands and Os d bands dominating the density of states at the Fermi energy $N(E_F)$ and they display almost the same lattice constant. For $\text{LaOs}_4\text{P}_{12}$, the highest contribution to $N(E_F)$ is from the P p band, the second highest from the Os d band, and the lowest from the La f band [37, 38]. The γ of $\text{LaOs}_4\text{P}_{12}$ is 20 mJ/molK² [35], which is comparable but moderately larger than that of $\text{CaOs}_4\text{P}_{12}$ with $\gamma_s \sim 16$ mJ/molK². $\text{LaOs}_4\text{P}_{12}$ is reported as metallic and its temperature-dependent resistivity, i.e., resistivity minus residual resistivity $\rho - \rho_0$ at 300 K is 0.35 mΩcm [39], while $\rho - \rho_0$ of $\text{CaOs}_4\text{P}_{12}$ is 1.4 mΩcm. The value of γ and resistivity are qualitatively consistent with each other but they display some

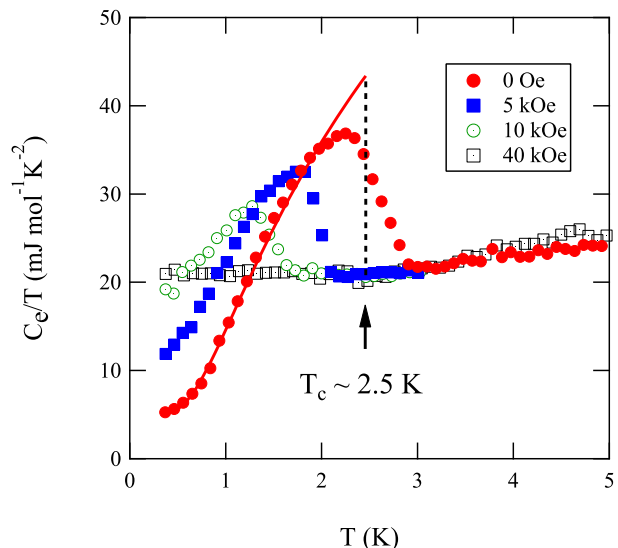


FIG. 5. (Color online) Electronic specific heat contribution C_e of $\text{CaOs}_4\text{P}_{12}$ under various fields, plotted as C_e/T vs T . The solid line represents the heat capacity based on the model of a spin-singlet fully gapped Bardeen-Cooper-Schrieffer (BCS) superconductor as numerically computed by Mühlischlegel (see text for details).

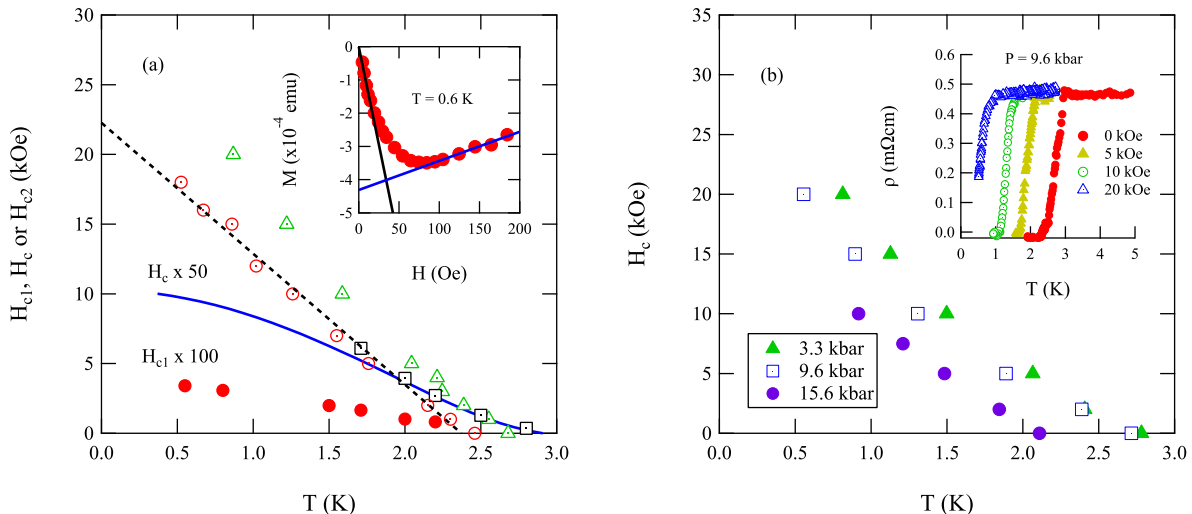


FIG. 6. (Color online) (a) The upper critical field defined by ρ (open triangle), C (open circle), and M (open square) vs. T . The thermodynamic critical field (solid line) and the lower critical field (filled circle) vs. T is also plotted, H_c is multiplied by 50, and H_{c1} is multiplied by 100 for clarity. The inset shows the field dependence of the magnetization of $\text{CaOs}_4\text{P}_{12}$ below 200 Oe at 0.6 K. The lower critical field is defined by the cross point of the solid lines (b) H_{c2} vs. T under pressure. The inset shows $\rho(T)$ under each field at 9.6 kbar.

quantitative difference. Several factors can influence the absolute resistivity values. One is the quality of the sample. $\text{LaOs}_4\text{P}_{12}$ and Sb-based alkaline-earth-filled skutterudites with $\rho_{300\text{K}} \approx 0.3\text{--}0.6$ m Ω cm can be synthesized at ambient pressure [8, 21–27], while As-based alkaline-earth-filled skutterudites with relatively high $\rho_{300\text{K}} \approx 1\text{--}5$ m Ω cm can only be synthesized at high pressures [18, 28–30]. The former compounds are supposed to be more stable than the latter, which might affect the resistivity. In addition, an effect of the small amount of secondary phases OsP_2 with 1 % and OsP_4 with 2 % cannot be excluded. Another factor is slightly different band structures. Sb-based alkaline-earth-filled skutterudites show almost the same resistivity, with $\rho_{300\text{K}} \approx 0.3\text{--}0.6$ m Ω cm, while the Sommerfeld value γ is strongly affected by transition element T , i.e., $\gamma \approx 90\text{--}120$ mJ/molK² for $T = \text{Fe}$, $\gamma \approx 10$ mJ/molK² for $T = \text{Ru}$, $\gamma \approx 40\text{--}50$ mJ/molK² for $T = \text{Os}$. These differences in γ are attributed to the density of states at the Fermi energy [27]. The y and z coordinates of the P site of $\text{CaOs}_4\text{P}_{12}$, which is in 24 (g) symmetry in space group $\text{Im}\bar{3}$, depends on the specific compound. As the p band from the P site is supposed to provide the highest contribution to the density of states at the Fermi energy, information on atomic position is needed for more detailed calculation of this effect.

The M - H curve at 0.6 K shows a linear dependence at low fields and deviates from linearity above 10 Oe, followed by a minimum at 80 Oe, as shown in the inset of Fig. 6 (a). The lower critical field H_{c1} is then determined from the cross point, as shown in the inset of Fig. 6 (a), where the lower line is an extrapolation of the linear

dependence in M - H . Figure 6 (a) shows the lower critical field H_{c1} , the thermodynamic critical field H_c , and the upper critical field H_{c2} versus T of $\text{CaOs}_4\text{P}_{12}$. $H_c(T)$ is obtained by integrating the entropy difference between the normal and superconducting states:

$$\frac{\mu_0 H_c^2(T)}{2} = \int_{T_c}^T \int_{T_c}^{T'} \frac{C_s - C_n}{T''} dT'' dT', \quad (1)$$

where C_s is the specific heat in the superconducting states and C_n is the specific heat in the normal states. The extrapolations of H_{c1} and H_c to $T = 0$ are $H_{c1}(0) = 40$ Oe and $H_c(0) = 210$ Oe, respectively. H_{c2} is derived from $\rho(H, T)$, $M(H, T)$, and $C(H, T)$. The $H_{c2}(T)$ deduced from the resistivity data is slightly higher than that from the specific heat data. Because the resistivity reflects surface conductivity, we define $H_{c2}(0)$ derived from the specific heat data. A linear extrapolation, as indicated by the dotted line, indicates $H_{c2}(0) = 22$ kOe. In the dirty limit, $H_{c2}(0)$ is given by $H_{c2}(0) = 0.693|dH_{c2}/dT|_{T_c} T_c$ for a type-II superconductor [40]. This equation yields a dirty limit estimate of $H_{c2}(0) \approx 16$ kOe for $\text{CaOs}_4\text{P}_{12}$.

The inset of Fig. 6 (b) illustrates the temperature-dependence of the electrical resistivity of $\text{CaOs}_4\text{P}_{12}$ measured under a pressure of 9.6 kbar, whereby zero resistivity is observed up to a field of 15 kOe. No drop of $\rho(T)$ due to superconductivity is observed above 25 kOe. Figure 6 (b) shows $H_{c2}(T)$ under pressure. Both $H_{c2}(0)$ and T_c monotonically decrease with applied pressure. Some skutterudite superconductors, however, exhibit a positive pressure dependence of T_c , similar to $\text{YFe}_4\text{P}_{12}$ or

LaFe₄P₁₂, while isostructural RT_4P_{12} ($R=Y, La, T=Ru, Os$) exhibits a negative pressure dependence [8, 9]. T_c of CaOs₄P₁₂ exhibits a negative pressure dependence as well. A negative pressure dependence of T_c or $H_{c2}(0)$ is the behavior expected for a BCS-type superconductor.

IV. DISCUSSION

TABLE I. Characteristic parameters of CaOs₄P₁₂ in comparison with LaOs₄P₁₂ [41, 42], Ba_{0.89}Ir₄P₁₂ [13], and BaPt₄Ge₁₂ [14]

	CaOs ₄ P ₁₂	LaOs ₄ P ₁₂	Ba _{0.89} Ir ₄ P ₁₂	BaPt ₄ Ge ₁₂
$a(\text{\AA})$	8.084	8.084	8.1071	8.6928
T_c (K)	2.5	1.8	5.6	5.35
H_c (Oe)	210	-	-	530
H_{c2} (kOe)	22	0.72	29	18
ξ (nm)	12	68	10.7	14
λ (nm)	400	-	-	320
κ	73	-	-	24
Θ_D (K)	560	532	368	247
$\Delta C/\gamma T_c$	1.4	-	1.04	1.35
λ_{ep}	0.47	0.4	0.62	0.7

Here, we discuss the superconducting properties of CaOs₄P₁₂. Filled skutterudite CaOs₄P₁₂ is a type-II superconductor because the susceptibilities in the FC and ZFC runs are markedly different. Table 1 lists some superconductivity parameters of CaOs₄P₁₂ together with LaOs₄P₁₂ and with alkaline-earth-filled skutterudites Ba_{0.89}Ir₄P₁₂ and BaPt₄Ge₁₂. The jump at the specific heat $\Delta C/\gamma T_c \approx 1.4$ closely agrees with the BCS value of 1.43. The critical temperature $T_c \approx 2.5$ K, as defined by the entropy balance of the specific heat. The lower, thermodynamic, and upper critical fields of CaOs₄P₁₂ are 40 Oe, 210 Oe, and 22 kOe, respectively. The Ginzburg-Landau parameter $\kappa = H_{c2}(0)/\sqrt{2}H_c(0)$ is deduced as 73, corroborating CaOs₄P₁₂ as a type-II superconductor. Although T_c of CaOs₄P₁₂ is less than half of that of BaPt₄Ge₁₂, $H_{c2}(0)$ of the former is larger than that of the latter. The higher $H_{c2}(0)$ implies a higher κ value. Even though $H_{c2}(0)$ is high despite a low T_c as compared to other alkaline-earth-filled skutterudites, it is less than the Pauli limiting field $H_P = 45$ kOe (deduced from $H_P = 1.83 T_c$); this refers to s -wave superconductivity. The penetration depth $\lambda = \sqrt{\Phi_0 \ln \kappa / 4\pi H_{c1}(0)}$ is deduced as

400 nm and the coherence length $\xi = \sqrt{\Phi_0 / 2\pi H_{c2}}$ is estimated to be 12 nm which is comparable with other alkaline-earth-filled skutterudites, Ba_{0.89}Ir₄P₁₂ with 10.7 nm and BaPt₄Ge₁₂ with 14 nm. The electron mean free path l was estimated to be 0.72 $[S/S_F]^{-1}$ nm from $l = 1.27 \times 10^4 [\rho n^{2/3} S/S_F]^{-1}$, where ρ , n , S , and S_F are the resistivity at 10 K, carrier concentration, Fermi surface, and Fermi surface of an electron gas of density n , respectively. We can assume the value of S/S_F in CaOs₄P₁₂ to be between 0.1 and 1.0, similar to La_{0.8}Rh₄P₁₂ [16], leading to a value of l between 0.72 and 7.2 nm. ξ is less than l , indicating that the sample is approximately in a dirty limit. The electron-phonon coupling constant λ_{ep} is calculated from the semiempirical formula proposed by McMillan [11], i.e.,

$$\lambda_{ep} = \frac{1.04 + \mu^* \ln(\Theta_D/1.45T_c)}{(1 - 0.62\mu^*) \ln(\Theta_D/1.45T_c) - 1.04} \approx 0.47, \quad (2)$$

where $\mu^* \approx 0.13$, $\Theta_D \approx 560$ K, and $T_c \approx 2.5$ K. It suggests that CaOs₄P₁₂ is a weakly coupled superconductor. Altogether, the superconducting parameters of CaOs₄P₁₂ obtained from this study are within the limit predicted by the BCS theory.

V. CONCLUSIONS

In this study, we succeeded in synthesizing CaOs₄P₁₂ using an HPHT procedure. A superconducting transition was found at $T_c \approx 2.5$ K; a significant fraction of the sample becomes superconducting. The lower, thermodynamic, and upper critical fields were 40 Oe, 210 Oe, and 22 kOe, respectively. The Ginsburg-Landau parameter, penetration depth, and coherence length are 73, 400 nm, and 12 nm, respectively. Superconductivity of CaOs₄P₁₂ can be regarded as type-II weakly coupled BCS-type superconductivity in the dirty limit. We suggest that CaOs₄P₁₂ is an s -wave superconductor. To confirm this, it is necessary to conduct microscopic studies using nuclear quadrupole resonance and nuclear magnetic resonance, as well as to investigate Fermi-surface properties by means of band structure calculations.

ACKNOWLEDGMENTS

A part of this study is supported by JSPS KAKENHI Grants No. JP23340092 and No. JP15K17687.

- [1] W. Jeitschko and D. J. Braun, Acta Crystallogr., Sect. B **33**, 3401–3406 (1977).
 [2] C. Sekine, T. Uchiumi, I. Shirotni, and T. Yagi, Phys. Rev. Lett. **79**, 3218 (1997).
 [3] N. Takeda and M. Ishikawa, Physica B **259–261**, 92–93 (1999).

- [4] K. Hachitani, H. Fukazawa, Y. Kohori, I. Watanabe, C. Sekine, and I. Shirotni, Phys. Rev. B **73**, 052408 (2006).
 [5] H. Sugawara, T. D. Matsuda, K. Abe, Y. Aoki, H. Sato, S. Nojiri, Y. Inada, R. Settai, and Y. Onuki, Phys. Rev. B **66**, 134411 (2002).

- [6] K. Iwasa, Y. Watanabe, K. Kuwahara, M. Kohgi, H. Sugawara, T. D. Matsuda, Y. Aoki, and H. Sato, *Physica B* **312–313**, 834–836 (2002).
- [7] E. D. Bauer, N. A. Frederick, P.-C. Ho, V. S. Zapf, and M. B. Maple, *Phys. Rev. B* **65**, 100506 (2002).
- [8] L. E. DeLong and G. P. Meisner, *Solid State Comm.* **53**, 119–123 (1985).
- [9] J.-G. Cheng, J.-S. Zhou, K. Matsubayashi, P. P. Kong, Y. Kubo, Y. Kawamura, C. Sekine, C. Q. Jin, J. B. Goodenough, and Y. Uwatoko, *Phys. Rev. B* **88**, 024514 (2013).
- [10] J. S. Schilling, *NATO Science Series* **48**, 345 (2001)
- [11] M. L. McMillan, *Phys. Rev.* **167**, 331 (1968).
- [12] N. Takeda, N. Hoshi, S. Yodono, R. Takeda, N. Kurotaki, and T. Nakano, *JPS Conf. Proc.* **3**, 017024 (2014).
- [13] Y. Qi, H. Lei, J. Guo, W. Shi, B. Yan, C. Felser, and H. Hosono, *J. Am. Chem. Soc.* **139**, 8106 (2017).
- [14] E. Bauer, A. Grytsiv, X. Q. Chen, N. Melnychenko-Koblyuk, G. Hilscher, H. Kaldarar, H. Michor, E. Royanian, G. Giester, M. Rotter, R. Podloucky, and P. Rogl, *Phys. Rev. Lett.* **99**, 217001 (2007).
- [15] R. Gumeniuk, W. Schnelle, H. Rosner, M. Nicklas, A. Leithe-Jasper, and Y. Grin, *Phys. Rev. Lett.* **100**, 10 (2008).
- [16] M. Imai, M. Akaishi, E. H. Sadki, T. Aoyagi, T. Kimura, and I. Shirovani, *Phys. Rev.* **75**, 184535 (2007).
- [17] S. Deminami, Y. Kawamura, Y. Q. Chen, M. Kanazawa, J. Hayashi, T. Kuzuya, K. Takeda, M. Matsuda, and C. Sekine, *J. Phys.: Conf. Ser.* **950**, 042032 (2017).
- [18] K. Nishine, Y. Kawamura, J. Hayashi, and C. Sekine, *J. J. Appl. Phys.* **56**, 05FB01 (2017).
- [19] C. Sekine, K. Akahira, K. Ito, and T. Yagi, *J. Phys. Soc. Jpn.* **78**, 093707 (2009).
- [20] K. Kihou, I. Shirovani, Y. Shimaya, C. Sekine, and T. Yagi, *Mater. Res. Bullet.* **39**, 317–325 (2004).
- [21] C. B. H. Evers, L. Boonk and W. Jeitschko, *Z. Anorg. Allg. Chem.* **620** 1028 (1994).
- [22] M. E. Danebrock, C. B. H. Evers and W. Jeitschko, *J. Phys. Chem. Solids* **57**, 381 (1996).
- [23] J.W. Kaiser and W. Jeitschko, *J. Alloys Compd.* **291**, 66–72 (1999)
- [24] A. Leithe-Jasper, W. Schnelle, H. Rosner, M. Baenitz, A. Rabis, A. A. Gippius, E. N. Morozova, H. Borrmann, U. Burkhardt, R. Ramlau, U. Schwarz, J. A. Mydosh, Y. Grin, V. Ksenofontov and S. Reiman, *Phys. Rev. B* **70**, 214418 (2004).
- [25] E. Matsuoka, K. Hayashi, A. Ikeda, K. Tanaka, T. Takabatake, and M. Matsumura, *J. Phys. Soc. Jpn.* **74**, 1382–1385 (2005).
- [26] E. Matsuoka, S. Narazu, K. Hayashi, K. Umeo, and T. Takabatake, *J. Phys. Soc. Jpn.* **75**, 014602 (2006).
- [27] T. Takabatake, E. Matsuoka, S. Narazu, K. Hayashi, S. Morimoto, T. Sasakawa, K. Umeo, and M. Sera, *Physica B* **383**, 93 (2006).
- [28] K. Takeda, K. Ito, J. Hayashi, C. Sekine, and T. Yagi, *J. Phys. Soc. Japan* **80**, SA029 (2011).
- [29] C. Sekine, T. Ishizaka, K. Nishine, Y. Kawamura, J. Hayashi, K. Takeda, H. Gotou, and Z. Hiroi, *Phys. Procedia.* **75**, 383–389 (2015).
- [30] K. Takeda, N. Hoshi, J. Hayashi, C. Sekine, S. Kagami, I. Shirovani, and T. Yagi, *J. Phys. Conf. Ser.* **215**, 012130 (2010).
- [31] R. Hauser, E. Bauer, and E. Gratz, *Phys. Rev. B* **57**, 2904 (1998).
- [32] D. E. Bugaris, C. D. Malliakas, D. P. Shoemaker, D. T. Do, D. Y. Chung, S. D. Mahanti, and M. G. Kanatzidis, *Inorg. Chem.* **53**, 9959–9968 (2014).
- [33] U. Florke and W. Jeitschko, *J. Less Common Met.* **86**, 247–253 (1982).
- [34] C. Sekine, K. Akita, N. Yanase, I. Shirovani, I. Inagawa, and C.-H. Lee, *Jpn. J. Appl. Phys.* **40**, 3326–3329 (2001).
- [35] K. Matsuhira, C. Sekine, M. Wakeshima, Y. Hinatsu, T. Namiki, K. Takeda, I. Shirovani, H. Sugawara, D. Kikuchi, and H. Sato, *J. Phys. Soc. Jpn.* **78**, 124601 (2009).
- [36] B. Mühlischlegel, *Z. Phys.* **155**, 313 (1959).
- [37] H. Sugawara, Y. Iwahashi, K. Magishi, T. Saito, K. Koyama, H. Harima, D. Kikuchi, H. Sato, T. Endo, R. Settai, Y. Onuki, N. Wada, H. Kotegawa, and T.C. Kobayashi, *J. Phys. Soc. Japan* **77**, Suppl. A 108–113 (2008).
- [38] H. Harima, K. Takegahara, *Phys. B Condens. Matter*, **403**, 906–908 (2008).
- [39] I. Shirovani, T. Adachi, K. Tachi, S. Todo, K. Nozawa, T. Yagi, and M. Kinoshita, *J. Phys. Chem. Solids* **57**, 211–216 (1996).
- [40] K. Maki, *Phys. Rev.* **148**, 362 (1966); N. R. Werthamer, E. Helfand, and P. C. Hohenberg, *Phys. Rev.* **147**, 295 (1966).
- [41] K. Matsuhira, Y. Doi, M. Wakeshima, Y. Hinatsu, K. Kihou, C. Sekine, and I. Shirovani: *Physica B* **359–361**, 977–979 (2005).
- [42] Y. Iwahashi, H. Sugawara, K. Magishi, T. Saito, K. Koyama, R. Settai, Y. Onuki, G. Giester, and P. Rogl, *J. Phys. Soc. Jpn.* **77** Suppl. A, 219 (2008).